W67.7: Coherence Preserving Tunable Coupler For 3D Cavities

Nick Materise[1], Srivatsan Chakram[2], Jens Koch[3], and Eliot Kapit[1]

[1]Department of Physics, Colorado School of Mines, Golden, CO 80401, USA

[2]Department of Physics & Astronomy, Rutgers University, Piscataway, NJ 08854, USA

[3]Department of Physics & Astronomy, Northwestern University, Evanston, IL 60208, USA

March 9, 2023

Introduction – Why 3D cavities?

N-modes with d-levels$= d^N$ large, compact Hilbert space[1]

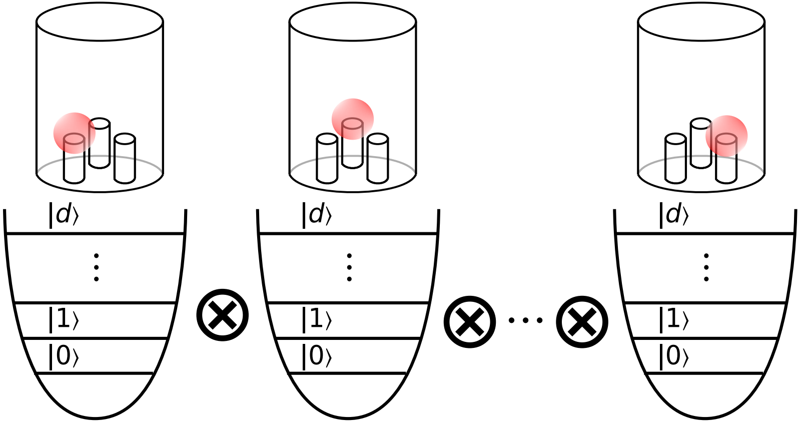

[1] Wang et al., Quantum Science and Technology **6**, 035015 (2021).

Introduction – Why 3D cavities?

Longest single microwave photon lifetimes in 3D cavities[2,3]

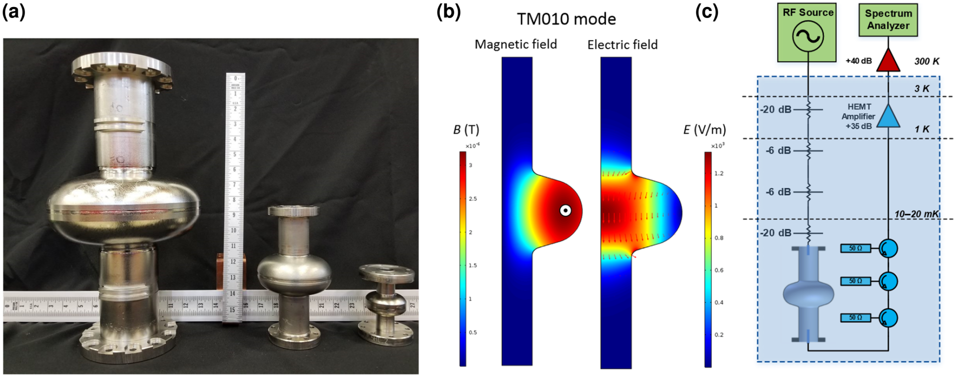

[2] Romanenko et al., Phys. Rev. Applied **13**, 034032 (2020).

[3] Milul et al., arXiv e-prints, arXiv:2302.06442 (2023).

Introduction – Why 3D cavities?

Bosonic error correction codes (GKP, binomial, cat codes, etc.)[4]

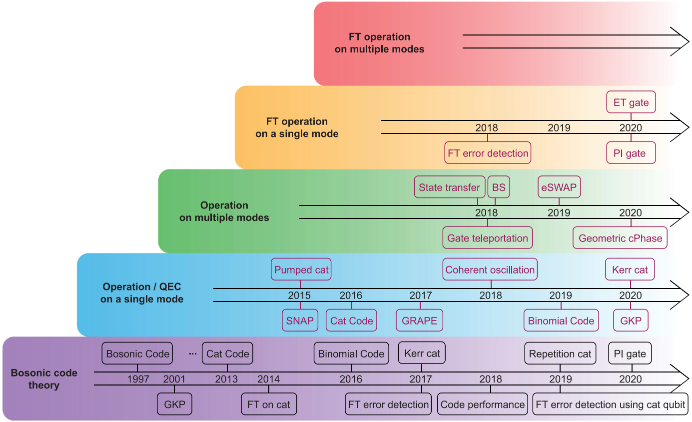

[4] Cai et al., Fundamental Research **1**, 50 (2021).

Introduction – Tunable couplers in 3D

Capacitive coupling – transmons (4WM)[5], SNAILs (3WM)[6]

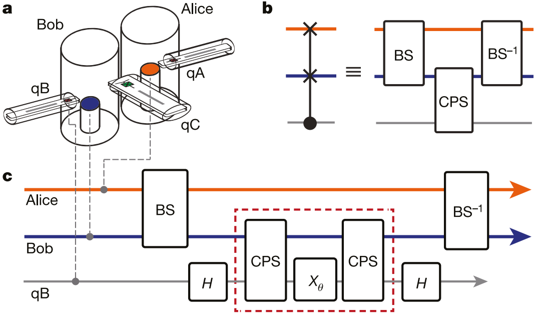

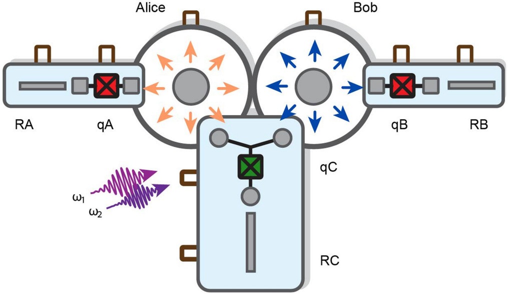

[5] Gao et al., Nature **566**, 509 (2019).

[6] Chapman et al., arXiv e-prints, arXiv:2212.11929 (2022).

Introduction – Tunable couplers in 3D

Capacitive coupling – transmons (4WM)[5], SNAILs (3WM)[6]

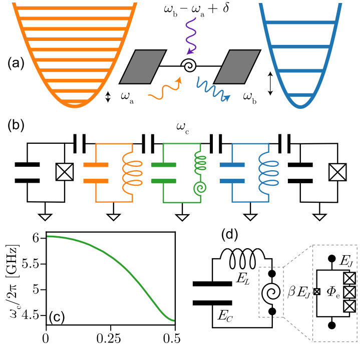

Flux Delivery

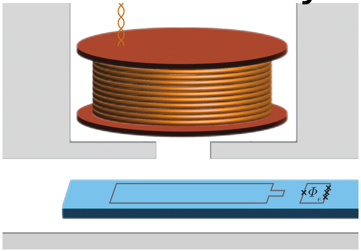

[5] Gao et al., Nature **566**, 509 (2019).

[6] Chapman et al., arXiv e-prints, arXiv:2212.11929 (2022).

Introduction – Tunable couplers in 3D

Capacitive coupling – SQUID tuned by cavity fields[7,8]

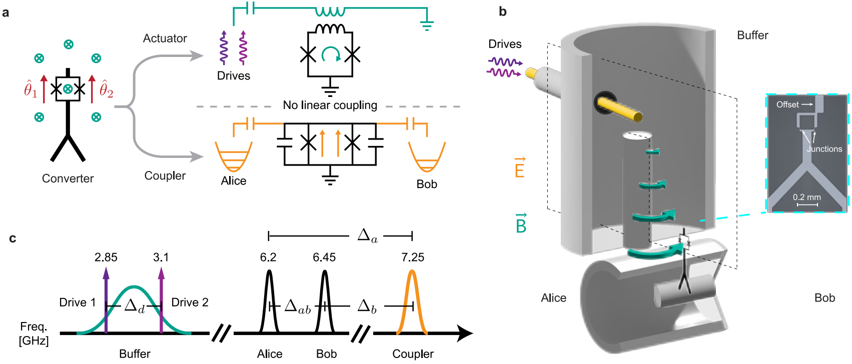

[7]March Meeting 2022, Q37.00001 : A novel package for fast-flux delivery in 3D

[8]Lu et al., arXiv e-prints, arXiv:2303.00959 (2023).

Introduction – Galvanic Coupling in 3D

- Galvanic coupling as a third coupling modality, beyond inductive and capacitive
  - Inspired by planar inductive-shunt-to-ground coupler[9]

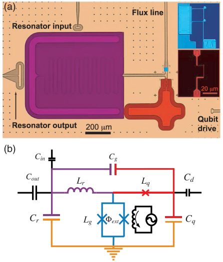

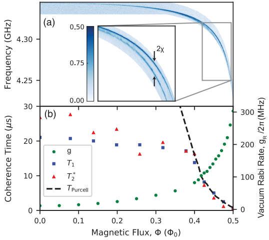

[9] Lu et al., Phys. Rev. Lett. **119**, 150502 (2017).

Introduction – Galvanic Coupling in 3D

- Galvanic coupling as a third coupling modality, beyond inductive and capacitive
  - Inspired by planar inductive-shunt-to-ground coupler[9]
  - Coupler mode placed far above cavity modes to reduce Purcell loss

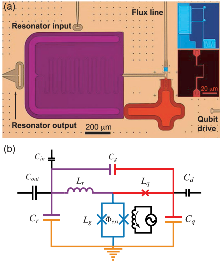

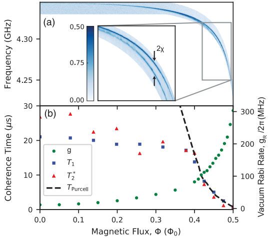

[9] Lu et al., Phys. Rev. Lett. **119**, 150502 (2017).

Introduction – Galvanic Coupling in 3D

- Galvanic coupling as a third coupling modality, beyond inductive and capacitive
  - Inspired by planar inductive-shunt-to-ground coupler[9]
  - Coupler mode placed far above cavity modes to reduce Purcell loss
  - Fast parametric operations (blue and red sidebands)

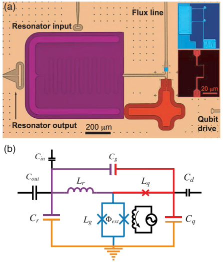

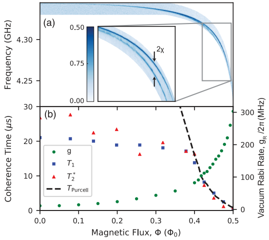

[9] Lu et al., Phys. Rev. Lett. **119**, 150502 (2017).

Introduction – Galvanic Coupling in 3D

- Galvanic coupling as a third coupling modality, beyond inductive and capacitive
  - Inspired by planar inductive-shunt-to-ground coupler[9]
  - Coupler mode placed far above cavity modes to reduce Purcell loss
  - Fast parametric operations (blue and red sidebands)
  - Design allows for recession of flux line, reducing control line noise

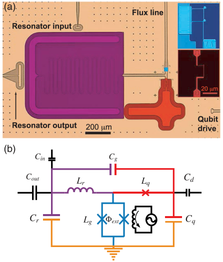

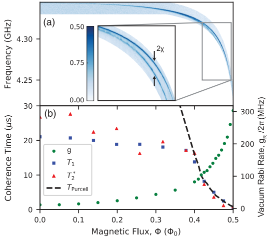

[9] Lu et al., Phys. Rev. Lett. **119**, 150502 (2017).

Introduction – Galvanic Coupling in 3D

- Galvanic coupling as a third coupling modality, beyond inductive and capacitive
  - Inspired by planar inductive-shunt-to-ground coupler[9]
  - Coupler mode placed far above cavity modes to reduce Purcell loss
  - Fast parametric operations (blue and red sidebands)
  - Design allows for recession of flux line, reducing control line noise
  - Poses new modeling challenges not encountered in 3D capacitive coupling designs

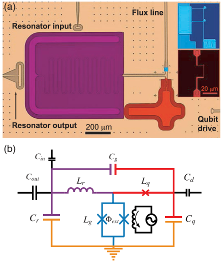

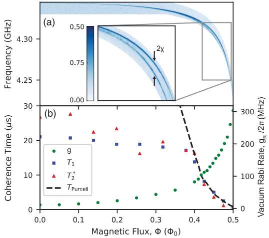

[9] Lu et al., Phys. Rev. Lett. **119**, 150502 (2017).

Modeling Approach: 1a. Black Box Quantization, Degenerate Cavities

- EPR[10] fails in galvanic coupling designs

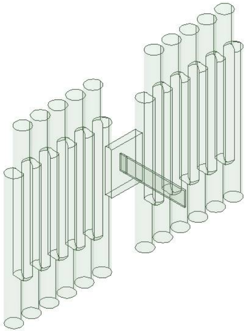

[10] Minev et al., arXiv: 2010.00620 [quant-ph] (2020).

[11] Nigg et al., Phys. Rev. Lett. **108**, 240502 (2012).

[12] Chakram et al., Phys. Rev. Lett. **127**, 107701 (2021).

Modeling Approach: 1a. Black Box Quantization, Degenerate Cavities

- EPR[10] fails in galvanic coupling designs
- Black box quantization approach[11]
- Degenerate flute cavity geometry + coupler slot[12]

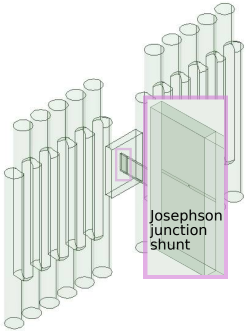

[10] Minev et al., arXiv: 2010.00620 [quant-ph] (2020).
[11] Nigg et al., Phys. Rev. Lett. **108**, 240502 (2012).
[12] Chakram et al., Phys. Rev. Lett. **127**, 107701 (2021).

Modeling Approach: 1a. Black Box Quantization, Degenerate Cavities

- EPR[10] fails in galvanic coupling designs
- Black box quantization approach[11]
- Degenerate flute cavity geometry + coupler slot[12]
- (Anti)symmetric modes (do not)do tune

Symmetric Mode
(tuning, antinode at coupler)

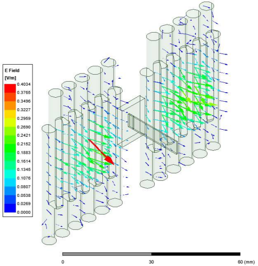

[10] Minev et al., arXiv: 2010.00620 [quant-ph] (2020).
[11] Nigg et al., Phys. Rev. Lett. **108**, 240502 (2012).
[12] Chakram et al., Phys. Rev. Lett. **127**, 107701 (2021).

Modeling Approach: 1a. Black Box Quantization, Degenerate Cavities

- EPR[10] fails in galvanic coupling designs
- Black box quantization approach[11]
- Degenerate flute cavity geometry + coupler slot[12]
- (Anti)symmetric modes (do not)do tune

Antisymmetric Mode
(no tuning, node at coupler)

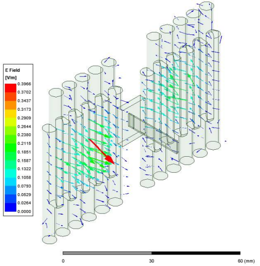

[10] Minev et al., arXiv: 2010.00620 [quant-ph] (2020).
[11] Nigg et al., Phys. Rev. Lett. **108**, 240502 (2012).
[12] Chakram et al., Phys. Rev. Lett. **127**, 107701 (2021).

Modeling Approach: 1a. Black Box Quantization, Degenerate Cavities

- EPR[10] fails in galvanic coupling designs
- Black box quantization approach[11]
- Degenerate flute cavity geometry + coupler slot[12]
- (Anti)symmetric modes (do not)do tune
- Add L_J by hand to admittances⇒modes

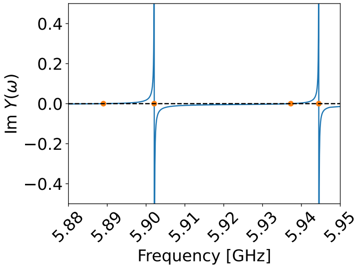

[10] Minev et al., arXiv: 2010.00620 [quant-ph] (2020).
[11] Nigg et al., Phys. Rev. Lett. **108**, 240502 (2012).
[12] Chakram et al., Phys. Rev. Lett. **127**, 107701 (2021).

Modeling Approach: 1a. Black Box Quantization, Degenerate Cavities

- EPR[10] fails in galvanic coupling designs
- Black box quantization approach[11]
- Degenerate flute cavity geometry + coupler slot[12]
- (Anti)symmetric modes (do not)do tune
- Add L_J by hand to admittances$\Rightarrow$modes

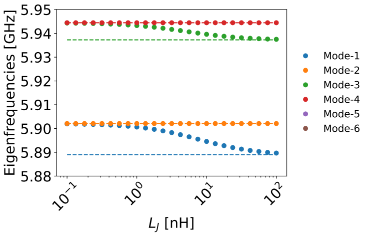

[10] Minev et al., arXiv: 2010.00620 [quant-ph] (2020).
[11] Nigg et al., Phys. Rev. Lett. **108**, 240502 (2012).
[12] Chakram et al., Phys. Rev. Lett. **127**, 107701 (2021).

Modeling Approach: 1a. Black Box Quantization, Degenerate Cavities

- EPR[10] fails in galvanic coupling designs
- Black box quantization approach[11]
- Degenerate flute cavity geometry + coupler slot[12]
- (Anti)symmetric modes (do not)do tune
- Add L_J by hand to admittances⇒modes
- Mode splitting from L_J sweep gives coupling

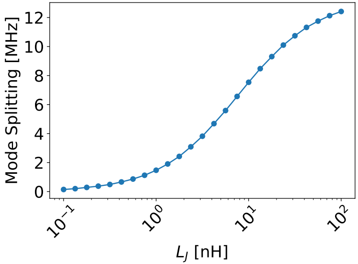

[10] Minev et al., arXiv: 2010.00620 [quant-ph] (2020).

[11] Nigg et al., Phys. Rev. Lett. **108**, 240502 (2012).

[12] Chakram et al., Phys. Rev. Lett. **127**, 107701 (2021).

Modeling Approach: 1a. Black Box Quantization, Degenerate Cavities

- EPR[10] fails in galvanic coupling designs
- Black box quantization approach[11]
- Degenerate flute cavity geometry + coupler slot[12]
- (Anti)symmetric modes (do not)do tune
- Add L_J by hand to admittances⇒modes
- Mode splitting from L_J sweep gives coupling
- Mode-T_1 vs. L_J

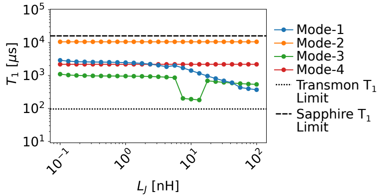

---

[10] Minev et al., arXiv: 2010.00620 [quant-ph] (2020).

[11] Nigg et al., Phys. Rev. Lett. **108**, 240502 (2012).

[12] Chakram et al., Phys. Rev. Lett. **127**, 107701 (2021).

Modeling Approach: 1b. Black Box Quantization, A/B Cavities

- Apply analysis to cavities ω_a, ω_b, coupler $\omega_c \gg \omega_a, \omega_b$

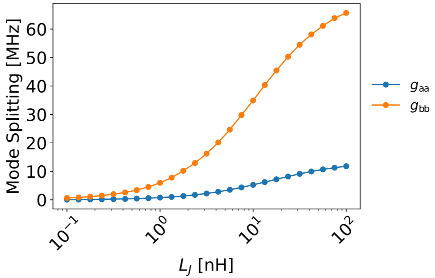

Modeling Approach: 1b. Black Box Quantization, A/B Cavities

- Apply analysis to cavities $\omega_a, \ \omega_b$, coupler $\omega_c \gg \omega_a, \omega_b$
- Two cavities with ω_a, $\Delta = |\omega_c - \omega_a|$, $g_{aa} = g_a^2/\Delta$

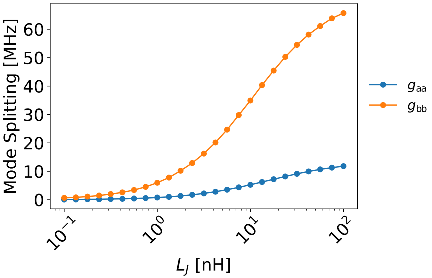

Modeling Approach: 1b. Black Box Quantization, A/B Cavities

- Apply analysis to cavities ω_a, ω_b, coupler $\omega_c \gg \omega_a, \omega_b$
- Two cavities with ω_a, $\Delta = |\omega_c - \omega_a|$, $g_{aa} = g_a^2/\Delta$
- Two cavities with ω_b, $\Delta = |\omega_c - \omega_b|$, $g_{bb} = g_b^2/\Delta$

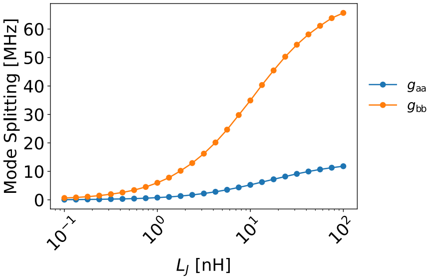

Modeling Approach: 1b. Black Box Quantization, A/B Cavities

- Apply analysis to cavities ω_a, ω_b, coupler $\omega_c \gg \omega_a, \omega_b$
- Two cavities with ω_a, $\Delta = |\omega_c - \omega_a|$, $g_{aa} = g_a^2/\Delta$
- Two cavities with ω_b, $\Delta = |\omega_c - \omega_b|$, $g_{bb} = g_b^2/\Delta$
- Two cavities ω_a, ω_b: $g_{ab} \approx g_a g_b/\Delta = \sqrt{g_{aa} g_{bb}}$

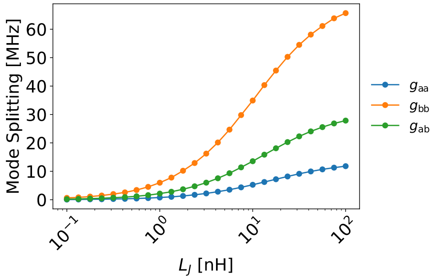

Modeling Approach: 1b. Black Box Quantization, A/B Cavities

- Apply analysis to cavities $\omega_a,\ \omega_b$, coupler $\omega_c \gg \omega_a, \omega_b$
- Two cavities with ω_a, $\Delta = |\omega_c - \omega_a|$, $g_{aa} = g_a^2/\Delta$
- Two cavities with ω_b, $\Delta = |\omega_c - \omega_b|$, $g_{bb} = g_b^2/\Delta$
- Two cavities ω_a, ω_b: $g_{ab} \approx g_a g_b/\Delta = \sqrt{g_{aa} g_{bb}}$
- Direct extraction of parametric rates from non-degenerate cavity simulations and overlap integrals of different field mode solutions across junction inductances

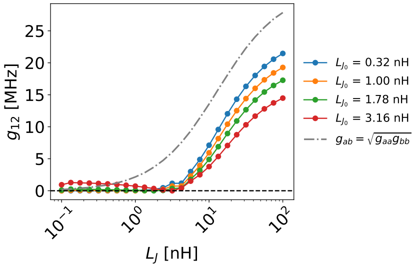

Modeling Approach: 1c. Flux Modulation

- Choose a bias point L_{J_0}

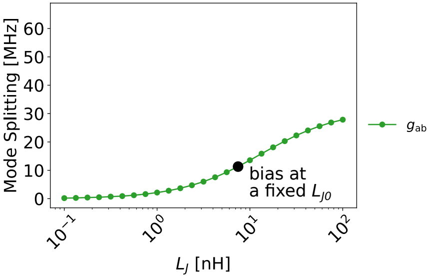

[13] Li et al., arXiv e-prints, arXiv:2302.06707 (2023).

[14] Q64.00009, Q64.000010 Star Code: Experimental Demonstration of Autonomous Error Correction with Two-Qutrits

Modeling Approach: 1c. Flux Modulation

- Choose a bias point L_{J_0}
- AC modulate flux at $\omega_{\mathrm{mod}} = \omega_a \pm \omega_b$ to generate beamsplitter, two mode squeezing operations[13,14]

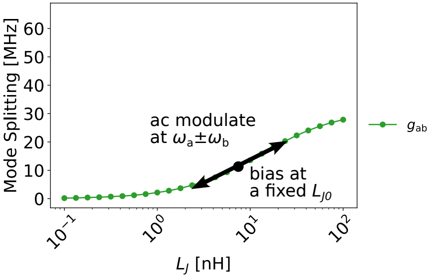

[13] Li et al., arXiv e-prints, arXiv:2302.06707 (2023).

[14] Q64.00009, Q64.000010 Star Code: Experimental Demonstration of Autonomous Error Correction with Two-Qutrits

Modeling Approach: 1c. Flux Modulation

- Choose a bias point L_{J_0}
- AC modulate flux at $\omega_{\mathrm{mod}} = \omega_a \pm \omega_b$ to generate beamsplitter, two mode squeezing operations[13,14]

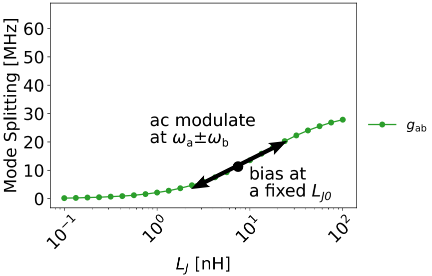

[13] Li et al., arXiv e-prints, arXiv:2302.06707 (2023).

[14] Q64.00009, Q64.000010 Star Code: Experimental Demonstration of Autonomous Error Correction with Two-Qutrits

Modeling Approach: 1c. Flux Modulation

- Choose a bias point L_{J_0}
- AC modulate flux at $\omega_{\mathrm{mod}} = \omega_a \pm \omega_b$ to generate beamsplitter, two mode squeezing operations[13,14]
- Parametric rates set by $1/2$ the modulation amplitude⇒several MHz

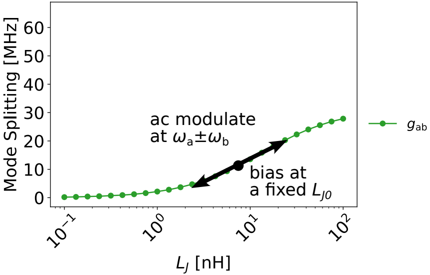

[13] Li et al., arXiv e-prints, arXiv:2302.06707 (2023).

[14] Q64.00009, Q64.000010 Star Code: Experimental Demonstration of Autonomous Error Correction with Two-Qutrits

Summary & Next Steps

- Designed a galvanic coupler design for flute cavities

Summary & Next Steps

- Designed a galvanic coupler design for flute cavities
- Simulated fast SWAP ratee, preserving high coherence of the cavity modes

Summary & Next Steps

- Designed a galvanic coupler design for flute cavities
- Simulated fast SWAP ratee, preserving high coherence of the cavity modes
- Work in progress on concrete design with recessed flux line and flux line filter

Summary & Next Steps

- Designed a galvanic coupler design for flute cavities
- Simulated fast SWAP ratee, preserving high coherence of the cavity modes
- Work in progress on concrete design with recessed flux line and flux line filter
- Experimental demonstrations to follow concrete designs

Summary & Next Steps

- Designed a galvanic coupler design for flute cavities
- Simulated fast SWAP ratee, preserving high coherence of the cavity modes
- Work in progress on concrete design with recessed flux line and flux line filter
- Experimental demonstrations to follow concrete designs
- Developed a method to extract parametric rates using field overlap integrals

Acknowledgements

- We thank Tanay Roy and others from the SQMS collaboration for fruitful discussions and feedback.
- We acknowledge funding from the Graduate Fellowship for STEM Diversity, NSF grant PHY-1653820, ARO grant No. W911NF-18-1-0125. This material is based upon work supported by the U.S. Department of Energy, Office of Science, National Quantum Information Science Research Centers, Superconducting Quantum Materials and Systems Center (SQMS) under contract number DE-AC02-07CH11359.

Black box quantization analysis details

- Start with admittance as seen by the junction and add in the JJ admittance, $T_{1,\mathrm{Purcell}} = 100\ \mu$s transmon lifetime included with R_J

$$Y_{\mathrm{tot}}(\omega) = Y_{\mathrm{HFSS}}(\omega) + Y_{\mathrm{JJ}}(\omega) \tag{1}$$

$$Y_{\mathrm{JJ}}(\omega) = j\omega C_J + \frac{1}{j\omega L_J} + \frac{1}{R_J} \tag{2}$$

$$T_{1,\mathrm{Purcell}} = \frac{C_J}{\mathrm{Re}\left[Y_{\mathrm{JJ}}(\omega)\right]} \Rightarrow R_J = \frac{C_J}{T_{1,\mathrm{Purcell}}} \tag{3}$$

[15] Nigg et al., Phys. Rev. Lett. **108**, 240502 (2012).

Black box quantization analysis details

- Start with admittance as seen by the junction and add in the JJ admittance, $T_{1,\mathrm{Purcell}} = 100$ μs transmon lifetime included with R_J

$$Y_{\mathrm{tot}}(\omega) = Y_{\mathrm{HFSS}}(\omega) + Y_{\mathrm{JJ}}(\omega) \tag{1}$$

$$Y_{\mathrm{JJ}}(\omega) = j\omega C_J + \frac{1}{j\omega L_J} + \frac{1}{R_J} \tag{2}$$

$$T_{1,\mathrm{Purcell}} = \frac{C_J}{\mathrm{Re}\left[Y_{\mathrm{JJ}}(\omega)\right]} \Rightarrow R_J = \frac{C_J}{T_{1,\mathrm{Purcell}}} \tag{3}$$

- Mode frequencies $\omega_p \ni \mathrm{Im}\left[Y_{\mathrm{tot}}(\omega)\right] = 0$, mode capacitances, resistances, losses[15]

$$C_p = \frac{1}{2}\frac{\mathrm{d}\mathrm{Im}\left[Y_{\mathrm{tot}}(\omega)\right]}{\mathrm{d}\omega}\bigg|_{\omega=\omega_p}, \quad R_p = \mathrm{Re}\left[Y_{\mathrm{tot}}(\omega_p)\right]^{-1}, \quad Q_p = \omega_p R_p C_p \tag{4}$$

[15] Nigg et al., Phys. Rev. Lett. **108**, 240502 (2012).

Derivation of electric field operator transformations–preliminaries

- $\mathbf{E}$-field operator expanded in $\mathbf{f}_k$ or $\widetilde{\mathbf{f}}_k$ eigenfunctions

$$\mathbf{E}(\mathbf{x}, L_J) = \sum_k \left[E_{k,0}(L_J) a_k(L_J) \mathbf{f}_k(\mathbf{x}, L_J) + \mathrm{h.c.}\right] = \sum_k \left[\widetilde{E}_{k,0}(L_{J_0}) \widetilde{a}_k(L_{J_0}) \widetilde{\mathbf{f}}_k(\mathbf{x}, L_{J_0}) + \mathrm{h.c.}\right] \tag{5}$$

Derivation of electric field operator transformations–preliminaries

- $\mathbf{E}$-field operator expanded in $\mathbf{f}_k$ or $\widetilde{\mathbf{f}}_k$ eigenfunctions

$$\mathbf{E}(\mathbf{x}, L_J) = \sum_k \left[E_{k,0}(L_J) a_k(L_J) \mathbf{f}_k(\mathbf{x}, L_J) + \mathrm{h.c.}\right] = \sum_k \left[\widetilde{E}_{k,0}(L_{J_0}) \widetilde{a}_k(L_{J_0}) \widetilde{\mathbf{f}}_k(\mathbf{x}, L_{J_0}) + \mathrm{h.c.}\right] \tag{5}$$

- Express $\mathbf{f}_k(\mathbf{x}, L_J)$ in terms of $\widetilde{\mathbf{f}}_k(\mathbf{x}, L_{J_0})$ and the converse

$$\mathbf{f}_k(\mathbf{x}, L_J) = \sum_{k'} A_{kk'}(L_J, L_{J_0}) \widetilde{\mathbf{f}}_{k'}(\mathbf{x}, L_{J_0}), \quad \widetilde{\mathbf{f}}_k(\mathbf{x}, L_{J_0}) = \sum_{k'} B_{kk'}(L_J, L_{J_0}) \mathbf{f}_{k'}(\mathbf{x}, L_J) \tag{6}$$

Derivation of electric field operator transformations–preliminaries

- $\mathbf{E}$-field operator expanded in $\mathbf{f}_k$ or $\widetilde{\mathbf{f}}_k$ eigenfunctions

$$\mathbf{E}(\mathbf{x}, L_J) = \sum_k \left[E_{k,0}(L_J) a_k(L_J) \mathbf{f}_k(\mathbf{x}, L_J) + \mathrm{h.c.}\right] = \sum_k \left[\widetilde{E}_{k,0}(L_{J_0}) \widetilde{a}_k(L_{J_0}) \widetilde{\mathbf{f}}_k(\mathbf{x}, L_{J_0}) + \mathrm{h.c.}\right] \tag{5}$$

- Express $\mathbf{f}_k(\mathbf{x}, L_J)$ in terms of $\widetilde{\mathbf{f}}_k(\mathbf{x}, L_{J_0})$ and the converse

$$\mathbf{f}_k(\mathbf{x}, L_J) = \sum_{k'} A_{kk'}(L_J, L_{J_0}) \widetilde{\mathbf{f}}_{k'}(\mathbf{x}, L_{J_0}), \quad \widetilde{\mathbf{f}}_k(\mathbf{x}, L_{J_0}) = \sum_{k'} B_{kk'}(L_J, L_{J_0}) \mathbf{f}_{k'}(\mathbf{x}, L_J) \tag{6}$$

- For real eigenfunctions, one can show that $B_{kk'} = A_{k'k}$

Derivation of electric field operator transformations–preliminaries

- $\mathbf{E}$-field operator expanded in $\mathbf{f}_k$ or $\widetilde{\mathbf{f}}_k$ eigenfunctions

$$\mathbf{E}(\mathbf{x}, L_J) = \sum_k \left[E_{k,0}(L_J) a_k(L_J) \mathbf{f}_k(\mathbf{x}, L_J) + \mathrm{h.c.}\right] = \sum_k \left[\widetilde{E}_{k,0}(L_{J_0}) \widetilde{a}_k(L_{J_0}) \widetilde{\mathbf{f}}_k(\mathbf{x}, L_{J_0}) + \mathrm{h.c.}\right] \tag{5}$$

- Express $\mathbf{f}_k(\mathbf{x}, L_J)$ in terms of $\widetilde{\mathbf{f}}_k(\mathbf{x}, L_{J_0})$ and the converse

$$\mathbf{f}_k(\mathbf{x}, L_J) = \sum_{k'} A_{kk'}(L_J, L_{J_0}) \widetilde{\mathbf{f}}_{k'}(\mathbf{x}, L_{J_0}), \quad \widetilde{\mathbf{f}}_k(\mathbf{x}, L_{J_0}) = \sum_{k'} B_{kk'}(L_J, L_{J_0}) \mathbf{f}_{k'}(\mathbf{x}, L_J) \tag{6}$$

- For real eigenfunctions, one can show that $B_{kk'} = A_{k'k}$
- Overlap integrals give $A_{kk'}$

$$A_{kk'}(L_J, L_{J_0}) = \frac{1}{V_{\mathrm{tot}}} \int_{V_{\mathrm{tot}}} \mathbf{f}_k(\mathbf{x}, L_J) \cdot \widetilde{\mathbf{f}}^{*}_{k'}(\mathbf{x}, L_{J_0}) d^3\mathbf{x} \tag{7}$$

Derivation of electric field operator transformations–preliminaries

- $\mathbf{E}$-field operator expanded in $\mathbf{f}_k$ or $\widetilde{\mathbf{f}}_k$ eigenfunctions

$$\mathbf{E}(\mathbf{x}, L_J) = \sum_k \left[E_{k,0}(L_J) a_k(L_J) \mathbf{f}_k(\mathbf{x}, L_J) + \mathrm{h.c.}\right] = \sum_k \left[\widetilde{E}_{k,0}(L_{J_0}) \widetilde{a}_k(L_{J_0}) \widetilde{\mathbf{f}}_k(\mathbf{x}, L_{J_0}) + \mathrm{h.c.}\right] \tag{5}$$

- Express $\mathbf{f}_k(\mathbf{x}, L_J)$ in terms of $\widetilde{\mathbf{f}}_k(\mathbf{x}, L_{J_0})$ and the converse

$$\mathbf{f}_k(\mathbf{x}, L_J) = \sum_{k'} A_{kk'}(L_J, L_{J_0}) \widetilde{\mathbf{f}}_{k'}(\mathbf{x}, L_{J_0}), \quad \widetilde{\mathbf{f}}_k(\mathbf{x}, L_{J_0}) = \sum_{k'} B_{kk'}(L_J, L_{J_0}) \mathbf{f}_{k'}(\mathbf{x}, L_J) \tag{6}$$

- For real eigenfunctions, one can show that $B_{kk'} = A_{k'k}$
- Substitute (6) into (5), solve for a_k in terms of $\widetilde{a}_k$

$$a_k(L_J) = \frac{1}{E_{k,0}(L_J)} \sum_{k'} \widetilde{E}_{k',0}(L_{J_0}) A_{kk'}(L_J, L_{J_0}) \widetilde{a}_{k'}(L_{J_0}) \tag{7}$$

Derivation of electric field operator transformations–Hamiltonian

- Substitute (7) into diagonal Hamiltonian

$$
\begin{aligned}
\mathcal{H} &= \sum_k \omega_k(L_J) \frac{1}{E_{k,0}^2(L_J)} \left[\sum_{k'} \widetilde{E}_{k',0}(L_{J_0}) \widetilde{a}_{k'}(L_{J_0}) A_{kk'}(L_J, L_{J_0}) \right]^\dagger \\
&\times \left[\sum_{k''} \widetilde{E}_{k'',0}(L_{J_0}) \widetilde{a}_{k''}(L_{J_0}) A_{kk''}(L_J, L_{J_0}) \right] \\
&= \sum_{k' k''} \sum_k \omega_k(L_J) \frac{1}{E_{k,0}^2(L_J)} \widetilde{E}_{k',0}(L_{J_0}) \widetilde{E}_{k'',0}(L_{J_0}) \\
&\times A_{kk'}^*(L_J, L_{J_0}) A_{kk''}(L_J, L_{J_0}) \widetilde{a}_{k'}^\dagger(L_{J_0}) \widetilde{a}_{k''}(L_{J_0})
\end{aligned} \tag{8}
$$

Derivation of electric field operator transformations–couplings & frequencies

- Beam splitter Hamiltonian

$$\mathcal{H} = \sum_{k} \widetilde{\omega}_k(L_J, L_{J_0})\widetilde{a}_k^\dagger(L_{J_0})\widetilde{a}_k(L_{J_0}) + \sum_{k \neq k'} g_{kk'}(L_J, L_{J_0})\widetilde{a}_k^\dagger(L_{J_0})\widetilde{a}_{k'}(L_{J_0}) \tag{9}$$

Derivation of electric field operator transformations–couplings & frequencies

- Beam splitter Hamiltonian

$$\mathcal{H} = \sum_k \widetilde{\omega}_k(L_J, L_{J_0})\widetilde{a}_k^\dagger(L_{J_0})\widetilde{a}_k(L_{J_0}) + \sum_{k\neq k'} g_{kk'}(L_J, L_{J_0})\widetilde{a}_k^\dagger(L_{J_0})\widetilde{a}_{k'}(L_{J_0}) \tag{9}$$

- Modified frequencies and couplings

$$\widetilde{\omega}_k(L_J, L_{J_0}) = \omega_k(L_{J_0})\sum_{k'} A^*_{k'k}(L_J, L_{J_0})A_{k'k}(L_J, L_{J_0}) \tag{10}$$

$$g_{kk'}(L_J, L_{J_0}) = \left[\omega_k(L_{J_0})\omega_{k'}(L_{J_0})\right]^{1/2}\sum_{k''} A^*_{k''k'}(L_J, L_{J_0})A_{k''k}(L_J, L_{J_0}) \tag{11}$$

Parametric Operation Derivations – Frequencies & Couplings

- Taking $L_J = L_J(t) = L_{J_0} + \delta L_J \sin(\omega_{mod} t)$, and expanding $\widetilde{\omega}_k$ about L_{J_0}, we have

$$\widetilde{\omega}_{k'}(L_J, L_{J_0}) \approx \widetilde{\omega}_{k'}(L_{J_0}, L_{J_0}) + \delta L_J \sin(\omega_{mod} t) \left.\frac{d\widetilde{\omega}_{k'}(L_J, L_{J_0})}{dL_J}\right|_{L_J = L_{J_0}}$$

$$= \omega_{k'}(L_{J_0}) + \frac{1}{2}\epsilon_{k'} \sin(\omega_{mod} t) \tag{12}$$

Parametric Operation Derivations – Frequencies & Couplings

- Taking $L_J = L_J(t) = L_{J_0} + \delta L_J \sin(\omega_{mod} t)$, and expanding $\widetilde{\omega}_k$ about L_{J_0}, we have

$$\begin{aligned}\widetilde{\omega}_{k'}(L_J, L_{J_0}) &\approx \widetilde{\omega}_{k'}(L_{J_0}, L_{J_0}) + \delta L_J \sin(\omega_{mod} t) \frac{d\widetilde{\omega}_{k'}(L_J, L_{J_0})}{dL_J}\bigg|_{L_J = L_{J_0}} \\ &= \omega_{k'}(L_{J_0}) + \frac{1}{2}\epsilon_{k'} \sin(\omega_{mod} t) \end{aligned} \tag{12}$$

- For the couplings $g_{k'k''}$, we find

$$\begin{aligned}g_{k'k''}(L_J, L_{J_0}) &\approx \cancelto{0}{g_{k'k''}(L_{J_0}, L_{J_0})} + \delta L_J \sin(\omega_{mod} t) \frac{dg_{k'k''}(L_J, L_{J_0})}{dL_J}\bigg|_{L_J = L_{J_0}} \\ &= \epsilon_{g_{k'k''}} \sin(\omega_{mod} t) \end{aligned} \tag{13}$$

Parametric Operation Derivations – Hamiltonian & Frame Transformation

- Substituting Eqs. (12) and (13) into the diagonal Hamiltonian, we write

$$\mathcal{H}(t) = \sum_{k'} \left(\omega_{k'}(L_{J_0}) + \frac{1}{2}\epsilon_{k'} \sin(\omega_{mod} t) \right) \tilde{a}^{\dagger}_{k'}(L_{J_0}) \tilde{a}_{k'}(L_{J_0}) + \sum_{k' \neq k''} \epsilon_{g_{k'k''}} \sin(\omega_{mod} t) \tilde{a}^{\dagger}_{k'}(L_{J_0}) \tilde{a}_{k''}(L_{J_0}) \tag{14}$$

[16] Strand et al., Phys. Rev. B **87**, 220505 (2013).

Parametric Operation Derivations – Hamiltonian & Frame Transformation

- Substituting Eqs. (12) and (13) into the diagonal Hamiltonian, we write

$$\mathcal{H}(t) = \sum_{k'} \left(\omega_{k'}(L_{J_0}) + \frac{1}{2}\epsilon_{k'} \sin(\omega_{mod} t) \right) \tilde{a}^{\dagger}_{k'}(L_{J_0}) \tilde{a}_{k'}(L_{J_0}) + \sum_{k' \neq k''} \epsilon_{g_{k'k''}} \sin(\omega_{mod} t) \tilde{a}^{\dagger}_{k'}(L_{J_0}) \tilde{a}_{k''}(L_{J_0}) \tag{14}$$

- To cancel the time dependence in the frequencies, we go to the rotating frame described by the unitary[16]

$$U(t) = \exp\left\{ i \sum_m \left[\left(\omega_m(L_{J_0}) t - \frac{\epsilon_m}{2\omega_{mod}} \cos(\omega_{mod} t) \right) \tilde{a}^{\dagger}_m(L_{J_0}) \tilde{a}_m(L_{J_0}) \right] \right\} \tag{15}$$

[16] Strand et al., Phys. Rev. B **87**, 220505 (2013).

Parametric Operation Derivations – Applying Transformation

- Jacobi-Anger theorem[17] to express $e^{\pm iz\cos(x)}$ in terms of Bessel functions $J_m(z)$

$$e^{\pm iz\cos(x)} = \sum_{m=-\infty}^{\infty} i^{\pm m} J_m(z) e^{\pm imx}. \tag{16}$$

[17] Abramowitz and Stegun, p. 358 (1965).

Parametric Operation Derivations – Applying Transformation

- Jacobi-Anger theorem[17] to express $e^{\pm iz\cos(x)}$ in terms of Bessel functions $J_m(z)$

$$e^{\pm iz\cos(x)} = \sum_{m=-\infty}^{\infty} i^{\pm m} J_m(z) e^{\pm imx}. \tag{16}$$

- The Hamiltonian in Eq. (14) transforms under $U(t)$ as

$$\mathcal{H}(t) \to \mathcal{H}' = U(t)\mathcal{H}(t)U^\dagger(t) - iU(t)\partial_t U^\dagger(t) \tag{17}$$

$$= \sum_{k' \neq k''} \epsilon_{g_{k'k''}} \sin(\omega_{mod} t) \tilde{a}^\dagger_{k'}(L_{J_0}) \tilde{a}_{k''}(L_{J_0}) e^{-i\Delta_{kk'} t}$$
$$\times \sum_{m,n=-\infty}^{\infty} i^{(m-n)} J_m\left(\frac{\epsilon_{k'}}{2\omega_{mod}}\right) J_n\left(\frac{\epsilon_{k''}}{2\omega_{mod}}\right) e^{i(m-n)\omega_{mod} t} \tag{18}$$

[17] Abramowitz and Stegun, p. 358 (1965).

Parametric Operation Derivations – Coupler Modulation

- Modulate the junction inductance at $\omega_{mod} = \Delta_{k'k''}$, and let $m = n$, the leading static component of Eq. (18) gives the effective couplings $g^{\text{eff}}_{k'k''}$

$$\mathcal{H}' \to \sum_{k' \neq k''} g^{\text{eff}}_{k'k''} \tilde{a}^{\dagger}_{k'}(L_{J_0}) \tag{19}$$

$$\boxed{g^{\text{eff}}_{k'k''} = \frac{\epsilon_{g_{k'k''}}}{2} \sum_{m=-\infty}^{\infty} J_m\left(\frac{\epsilon_{k'}}{2\omega_{mod}}\right) J_m\left(\frac{\epsilon_{k''}}{2\omega_{mod}}\right) \to \frac{\epsilon_{g_{k'k''}}}{2}, \epsilon_{k'} = \epsilon_{k''}} \tag{20}$$

Detailed Field Analysis Results – Matrices

Field Overlap Matrix

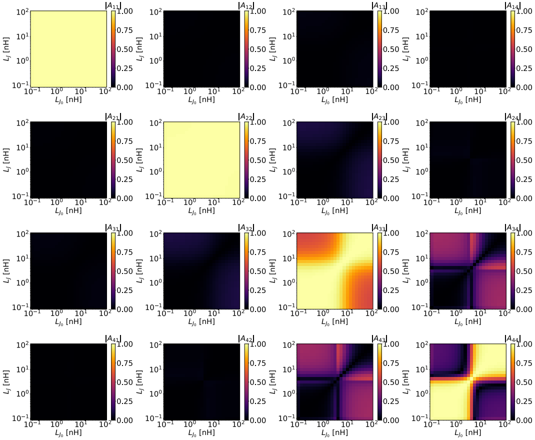

Beamsplitter Coupling Matrix

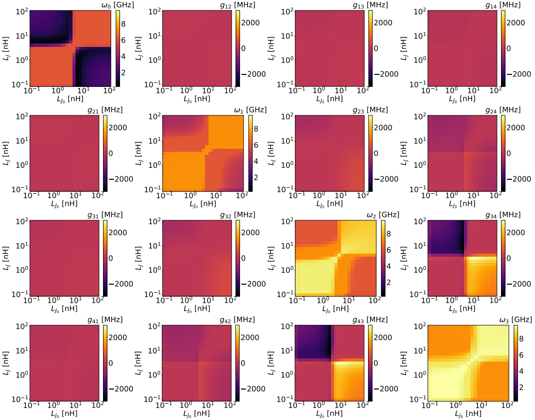

Detailed Field Analysis Results – Couplings

- Small L_{J_0} geometric mean underestimates

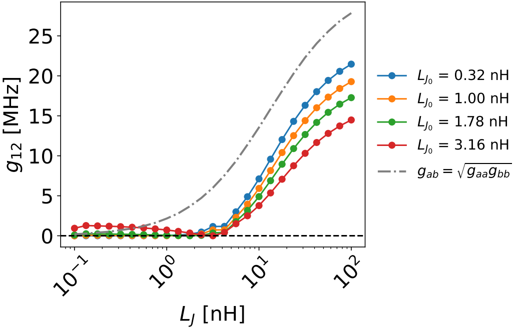

Detailed Field Analysis Results – Couplings

- Small L_{J_0} geometric mean underestimates
- Large L_{J_0} geometric mean agrees near $L_J = 5$ nH

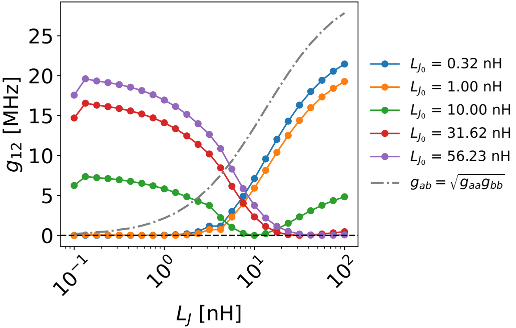

Detailed Field Analysis Results – Couplings

- Small L_{J_0} geometric mean underestimates
- Large L_{J_0} geometric mean agrees near $L_J = 5$ nH
- All g_{12} pass through zero at $L_J = L_{J_0}$ by orthogonality of field eigenfunctions

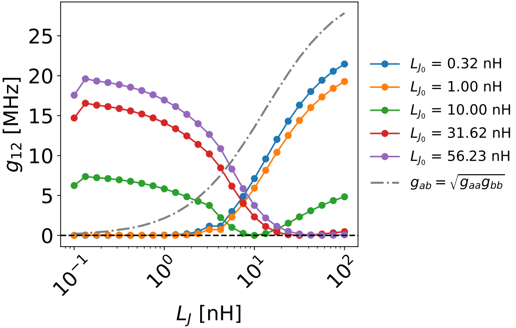

Mode Anharmonicities

Work in progress to understand large mode anharmonicities

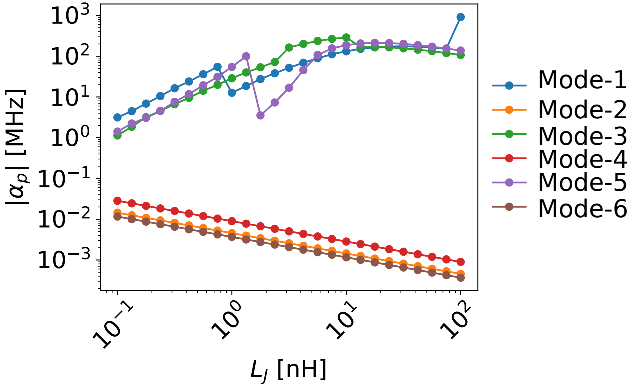

Field integration–numerical details

- Approximate integral by a sum

$$\int_V f(\mathbf{x})\mathrm{d}^3\mathbf{x} \approx \sum_{m=1}^{N_{\mathrm{elem}}} \sum_{n=1}^{N_{\mathrm{nodes}}} f(\mathbf{x}_{m,n})\Delta x_{1,n}\Delta x_{2,n}\Delta x_{3,n}$$
$$= \sum_{mn} f(\mathbf{x}_{m,n}) V_n \tag{21}$$

Field integration–numerical details

- Approximate integral by a sum

$$\int_V f(\mathbf{x})\mathrm{d}^3\mathbf{x} \approx \sum_{m=1}^{N_{\mathrm{elem}}} \sum_{n=1}^{N_{\mathrm{nodes}}} f(\mathbf{x}_{m,n})\Delta x_{1,n}\Delta x_{2,n}\Delta x_{3,n} = \sum_{mn} f(\mathbf{x}_{m,n}) V_n \tag{21}$$

- HFSS tetrahedral mesh node indices

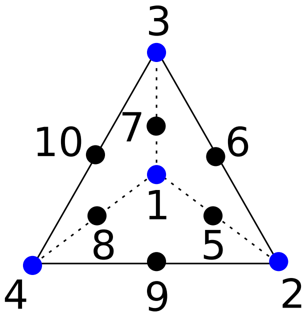

Field integration–numerical details

- Approximate integral by a sum

$$\int_V f(\mathbf{x})\mathrm{d}^3\mathbf{x} \approx \sum_{m=1}^{N_\text{elem}} \sum_{n=1}^{N_\text{nodes}} f(\mathbf{x}_{m,n})\Delta x_{1,n}\Delta x_{2,n}\Delta x_{3,n} = \sum_{mn} f(\mathbf{x}_{m,n})V_n \tag{21}$$

- HFSS tetrahedral mesh node indices
- Volume of tetrahedron from vertices v_1, v_2, v_3, v_4

$$\frac{1}{6}\det\begin{pmatrix} v_{1,1}-v_{4,1} & v_{2,1}-v_{4,1} & v_{3,1}-v_{4,1} \\ v_{1,2}-v_{4,2} & v_{2,2}-v_{4,2} & v_{3,2}-v_{4,2} \\ v_{1,3}-v_{4,3} & v_{2,3}-v_{4,3} & v_{3,3}-v_{4,3} \end{pmatrix}$$

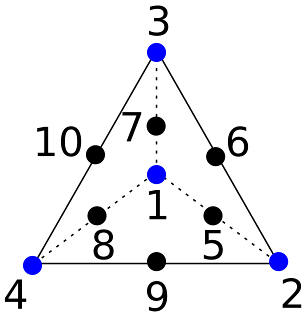

References

[1] Haozhi Wang et al. "Cryogenic single-port calibration for superconducting microwave resonator measurements". In: *Quantum Science and Technology* 6.3 (June 2021), 035015. DOI: 10.1088/2058-9565/ac070e.

[2] A. Romanenko et al. "Three-Dimensional Superconducting Resonators at $T < 20$ mK with Photon Lifetimes up to $\tau = 2$ s". In: *Phys. Rev. Applied* 13 (3 Mar. 2020), 034032. DOI: 10.1103/PhysRevApplied.13.034032.

[3] Ofir Milul et al. "A superconducting quantum memory with tens of milliseconds coherence time". In: *arXiv e-prints*, arXiv:2302.06442 (Feb. 2023), arXiv:2302.06442. DOI: 10.48550/arXiv.2302.06442. arXiv: 2302.06442 [quant-ph].

[4] Weizhou Cai et al. "Bosonic quantum error correction codes in superconducting quantum circuits". In: *Fundamental Research* 1.1 (2021), 50. DOI: https://doi.org/10.1016/j.fmre.2020.12.006.

[5] Yvonne Y. Gao et al. "Entanglement of bosonic modes through an engineered exchange interaction". In: *Nature* 566.7745 (Feb. 2019), 509. DOI: 10.1038/s41586-019-0970-4.

[6] Benjamin J. Chapman et al. "A high on-off ratio beamsplitter interaction for gates on bosonically encoded qubits". In: *arXiv e-prints*, arXiv:2212.11929 (Dec. 2022), arXiv:2212.11929. arXiv: 2212.11929 [quant-ph].

[7] Yao Lu et al. "A high-fidelity microwave beamsplitter with a parity-protected converter". In: *arXiv e-prints*, arXiv:2303.00959 (Mar. 2023), arXiv:2303.00959. DOI: 10.48550/arXiv.2303.00959. arXiv: 2303.00959 [quant-ph].

[8] Yao Lu et al. "Universal Stabilization of a Parametrically Coupled Qubit". In: *Phys. Rev. Lett.* 119 (15 Oct. 2017), 150502. DOI: 10.1103/PhysRevLett.119.150502.

[9] Zlatko K. Minev et al. *Energy-participation quantization of Josephson circuits*. 2020. arXiv: 2010.00620 [quant-ph].

[10] Simon E. Nigg et al. "Black-Box Superconducting Circuit Quantization". In: *Phys. Rev. Lett.* 108 (24 June 2012), 240502. DOI: 10.1103/PhysRevLett.108.240502.

[11] Srivatsan Chakram et al. "Seamless High-Q Microwave Cavities for Multimode Circuit Quantum Electrodynamics". In: *Phys. Rev. Lett.* 127 (10 Aug. 2021), 107701. DOI: 10.1103/PhysRevLett.127.107701.

[12] Ziqian Li et al. "Autonomous error correction of a single logical qubit using two transmons". In: *arXiv e-prints*, arXiv:2302.06707 (Feb. 2023), arXiv:2302.06707. DOI: 10.48550/arXiv.2302.06707. arXiv: 2302.06707 [quant-ph].

[13] J. D. Strand et al. "First-order sideband transitions with flux-driven asymmetric transmon qubits". In: *Phys. Rev. B* 87 (22 June 2013), 220505. DOI: 10.1103/PhysRevB.87.220505.

[14] M. Abramowitz and I.A. Stegun. "Handbook of Mathematical Functions: With Formulas, Graphs, and Mathematical Tables". In: Applied mathematics series. Dover Publications, 1965. Chap. 9, 358.